Regulation of Aquaporin 3 Expression by the AhR Pathway Is Critical to Cell Migration

Linh-Chi Bui, Céline Tomkiewicz, Stephane Pierre, Aline Chevallier, Robert Barouki, Xavier Coumoul

OXFORD UNIVERSITY PRESS | Toxicological Sciences

Regulation of Aquaporin 3 expression by the AhR pathway is critical to cell migration

Journal:	*Toxicological Sciences*
Manuscript ID:	TOXSCI-15-0450.R1
Manuscript Type:	Research Article
Date Submitted by the Author:	n/a
Complete List of Authors:	BUI, Linh-Chi; Université Paris Diderot, Sorbonne Paris Cité, CNRS UMR 8251, Biologie Fonctionnelle et Adaptative, TOMKIEWICZ, Céline; INSERM UMR-S 1124, Université Paris Descartes, Sorbonne Paris Cité, PIERRE, Stephane; INSERM UMR-S 1124, Université Paris Descartes, Sorbonne Paris Cité, CHEVALLIER, Aline; INSERM UMR-S 1124, Université Paris Descartes, Sorbonne Paris Cité, BAROUKI, Robert; INSERM UMR-S 1124, Université Paris Descartes, Sorbonne Paris Cité, COUMOUL, Xavier; INSERM UMR-S 1124, Université Paris Descartes, Sorbonne Paris Cité,
Key Words:	dioxin < Agents, receptor; aryl hydrocarbon < Gene Expression/Regulation, signal transduction < Gene Expression/Regulation, transcription factors < Gene Expression/Regulation, liver < Systems Toxicology, cell culture < In Vitro and Altenatives
Society of Toxicology Specialty Section Subject Area:	Mechanisms [116]

Title Page

Title: Regulation of Aquaporin 3 expression by the AhR pathway is critical to cell migration

Authors: Bui Linh-Chi[‡†*$], Tomkiewicz Céline[†*$], Pierre Stephane[†*], Chevallier Aline[†*], Barouki Robert[†*¶], Coumoul Xavier[†*]

[*] INSERM UMR-S 1124, Toxicologie Pharmacologie et Signalisation cellulaire, 45 rue des Saints-Pères, 75006 Paris, France

[†] Université Paris Descartes, Sorbonne Paris Cité, 45 rue des Saints-Pères, 75006 Paris, France

[‡] Université Paris Diderot, Sorbonne Paris Cité, CNRS UMR 8251, Biologie Fonctionnelle et Adaptative, 4 rue Marie-Andrée Lagroua Weill Hallé, 75213 Paris, France

[¶] AP-HP, Hôpital Necker-Enfants Malades, Service de biochimie métabolique, 149 rue de Sèvres, 75743 Paris, France

$ These authors contributed equally to this work.

To whom correspondence should be addressed at INSERM UMR-S 1124, 45 rue des Saints-Pères, 75006 Paris, France, phone: +33142863359; fax : +33142863868 ; email : xavier.coumoul@parisdescartes.fr

Running title: AQP3, a transcriptional AhR target, regulates cell migration

Abstract

The regulation of cell migration is a key factor for the dissemination of metastatic cells during tumor progression. Aquaporins are membrane channels which allow transmembrane fluxes of water and glycerol in cells in a variety of mammalian tissues. Here, we show that AQP3, which has been incriminated in cancer progression, is regulated by the AhR, or dioxin receptor. AhR is a transcription factor which is triggered in response to environmental pollutants and it has been shown to regulate several cellular processes including cell migration and plasticity. *In vivo*, upon exposure to the AhR ligand, 2,3,7,8-tetrachlorodibenzo-p-dioxin (TCDD), the expression of AQP3 is increased significantly in several murine tissues including the liver. *In vitro,* treatment of human HepG2 cells with TCDD also increased the expression of AQP3 mRNA and protein. These effects resulted from the activation of AhR as shown by RNA interference, chromatin immunoprecipitation and the use of several AhR ligands. Immunofluorescence and real-time analysis of cell migration (XCelligence) demonstrated that knockdown of AQP3 mRNA using small interfering RNA impairs the remodeling of cell shape and the triggering of cell migration that is induced by TCDD. Our work reveals, for the first time, a link between exposure to pollutant and the induction of an aquaporin which has been suspected to play a role during metastasis.

Keywords: Aryl hydrocarbon Receptor; PAHs; Aquaporin; cell migration ; transcription; dioxin; AQP3

Introduction

The aryl hydrocarbon receptor (AhR) is a member of the Per-ARNT-Sim family of proteins and has been described primarily as a sensor of xenobiotics which include dioxins, polycyclic aromatic hydrocarbons and polychlorinated biphenyls. It is a transcription factor which positively regulates the expression of xenobiotic metabolism enzymes which allow for the detoxication of AhR ligands (Coumoul et al., 2001). Although this elegant mechanism has been characterized extensively, other functions of the AhR have subsequently emerged during the last decade due to large-scale studies or the use of knock-out models (Barouki et al., 2007; Ma et al., 2009).

Recently, we and others have shown that the AhR regulates cell migration and invasion (Carvajal-Gonzalez et al., 2009; Barouki and Coumoul, 2010; Rico-Leo et al., 2013; Rey-Barroso et al., 2014). Interestingly, altered migration is observed not only upon treatment of primary cells or cell lines with AhR ligands but also in knockout cell lines as the result of the absence of the receptor. *In vivo* studies also suggest that the AhR is a critical regulator of cell migration and invasion (Carvajal-Gonzalez et al., 2009; Pierre et al., 2014). We have identified several of the cellular targets of the AhR pathway which are involved in this regulation. Some of them are critical mainly for cell proliferation (Son of Sevenless 1 or Sos1) whereas others affect cell migration (Human Enhancer of Filamentation 1 or HEF1, also known as Cas-L or NEDD9) (Bui et al., 2009; Pierre et al., 2011). In addition to the well described genomic pathway, AhR may act via non-genomic pathways involving Src and Focal Adhesion Kinase (FAK) to regulate cell morphology and migration. The genomic and non-genomic pathways could converge functionally since they have common targets such as the Hef1 protein, which is part of the integrin/FAK signaling

pathway. However, although this pathway appears to be necessary, there is no evidence to show that it is sufficient by itself to mediate the effects of dioxin.

Our whole genome transcriptome analyses also have demonstrated that the expression of aquaporin 3 (AQP3) is increased significantly in HepG2 cells following their exposure to dioxin. Aquaporins are a family of membrane water/glycerol channels which are involved in physiology and pathophysiology (Verkman et al., 2014). Their structures allow fast transfer of water and small molecules (including glycerol for some members of the family) across biological membranes. In microorgansims, these proteins regulate the adaptation to osmotic shock and rapid freezing. In mammals, which are the organisms the most studied, they regulate cell behavior (migration, proliferation), metabolism and transport (Verkman et al., 2014). Indeed, recently, a role *in vivo* was demonstrated for AQP in cell migration and, potentially, in cell metastasis (Verkman et al., 2014).

In this article, we show that AQP3 is a transcriptional target of the AhR and its ligands both *in vivo* in mice *and in vitro*, in human cells. Moreover, we show that the induction of AQP3 is critical for TCDD-induced morphological and migratory changes.

Materials and methods

Cell culture

Human hepatoblastoma HepG2 and mammary MDA-MB-231 cells were cultured at 37°C in Dulbecco's minimal essential medium (DMEM) complemented with nonessential amino acids, supplemented with 10% fetal bovine serum, 200 U/ml penicillin, 50 mg/ml streptomycin (Invitrogen, Cergy-Pontoise, France) and 0.5 mg/ml amphotericin B (Bristol-Myers Squibb Co., Stamford, CT, USA) in a humidified atmosphere in 5% CO_2. One day before exposure to various concentrations of TCDD, the cells were cultivated in DMEM without phenol red supplemented with 3% charcoal-treated (desteroidized) calf serum and maintained in this medium during all treatments. The human epidermal keratinocytes YF23 were cultured according to Vanhoutteghem A. *et al* (Vanhoutteghem and Djian, 2004).

TCDD was purchased from LCG Promochem (Molsheim, France). Benzo(a)pyrene, 3-methylcholanthrene, resveratrol and quercetin were purchased from Sigma-Aldrich (St Louis, MO, US).

Animals, treatments, and tissue extraction

Male C57BL/6J mice (Janvier, France) were housed in temperature and humidity-controlled rooms, kept on a 12-hour light-dark cycle, and provided unrestricted amounts of food and water chow diet (V153x R/M-H, Ssniff GmbH). The animal treatment protocol was approved by the bioethics committee of Paris Descartes University (authorization no. CEEA34.MA.003.12.) and all animals received humane care according to the Guide for the Care and the Use of Laboratory Animals (NIH publication 86-23 revised 1985).

Male mice (7 weeks old, n=5) were injected IP with 200 µl of either TCDD (25 µg/kg body weight) or the vehicle (corn oil). This amount of TCDD leads, after 48h, to a blood concentration of TCDD ranging from 100 to 1000 ppt according to Emond's physiologically based pharmacokinetic model. Those concentrations mimic a high TCDD contamination. The treatment consisted of injections of TCDD or corn oil on day 0 and 7 and the mice were sacrificed on day 14. The tissues (skin, liver, kidney, heart, lung, cerebellum, cortex) were removed immediately and frozen in liquid nitrogen.

Chromatin Immunoprecipitation (ChIP)

HepG2 cells were seeded in 150-mm-diameter dishes 48h before being processed for ChIP (approximately $20x10^6$ cells per dish). Cells were exposed to TCDD (25nM) for 15 or 45 minutes in DMEM without phenol red supplemented with 3% charcoal-treated calf serum (see above). The cells were rinsed with 37°C phosphate-buffered saline (PBS) and nuclear proteins were cross-linked to DNA by adding formaldehyde to a final concentration of 1% for 10 min at 37°C. Cross-linking was stopped by adding glycine to a final concentration of 0.125M for 5 min on ice. The cells were collected in ice cold PBS supplemented with complete protease inhibitor tablets (Cat. 1873580, Roche, Mannheim, Germany) and pelleted. Pellets were lysed in 500µl of lysis buffer (1% SDS, 10mM EDTA, 50mM Tris-HCl, pH 8.1, and protease inhibitors) for 10 min on ice. This solution was sonicated 10 times for 30s each at the high position with a Dismembrator 300 (Fisher). The soluble chromatin was then centrifuged at 12000 rpm for 15 min at 4°C and was diluted 1:10 in ChIP dilution buffer (0.01% SDS, 1.1% Triton X-100, 1.2mM EDTA, 16.7mM Tris-HCl, pH 8.1, 167mM NaCl, and protease inhibitors). An aliquot of the soluble chromatin was set

aside as the input fraction. Diluted chromatin was pre-cleared with protein A/G Plus agarose (Cat Sc-2003, Santa Cruz) at 4°C for 2h with rotation. Protein A/G agarose beads were pelleted, the supernatant was transferred to a new tube and incubated with 5 µg of anti-AhR antibody (Cat SA-210, BioMol) or 5 µg of normal rabbit IgG (negative control, Cat Sc-2027, Santa Cruz) for immunoprecipitation overnight at 4°C with rotation. After immunoprecipitation, fresh protein A/G agarose beads were added and incubated for 1h at 4°C with rotation. Agarose beads were pelleted and washed sequentially for 5 min with the following buffers: once with Buffer I (0.1% SDS, 1% Triton X-100, 2mM EDTA, 200mM Tris-HCl, pH 8.1, 150mM NaCl, and protease inhibitors), twice with Buffer II (0.1% SDS, 1% Triton X-100, 2mM EDTA, 200mM Tris-HCl, pH 8.1, 500mM NaCl, and protease inhibitors) and twice with Buffer III (0.25M LiCl, 1% NP-40, 1% deoxycholate, 1mM EDTA, 10mM Tris-HCl, pH 8.1). Protein-DNA complexes were eluted by adding 400µl of elution buffer (1% SDS, 0.1M NaHCO3, protease inhibitors), 20min at room temperature with rotation (input samples were included). The cross-linking was reversed by adding NaCl to a final concentration of 0.2M and incubating overnight at 65°C. The DNA was purified using a PCR purification kit (Cat 28106, Qiagen) and eluted in 25µl.

We used the UCSC Genome Bioinformatics site (http://genome.ucsc.edu) and the MatInspector software (http://www.genomatix.de/online_help/help_matinspector/) to characterize a potential XRE inside the human AQP3 promoter sequence:

A potential XRE site was located in the region (-1052/-887: TGGGCATGGTGGTGTGCACCTGTAATCCCAGCTAATCGGGAGGCTGAAGCAGG AGAATCACTTGAACCTGGGAGGTGGAGGTTGCAGGGAGCCGAGAT***CACGC***CAT TGCACTCCACCTAGGCGACAGAGAGAGACTCCGTCTAAAAAAAAAAAAGAGACA GACTC) and is represented in **bold** and *italics* (-954/-950)

ChIP DNA was analyzed by quantitative PCR using the specific primers covering the region -1052-887 bp of the human AQP3 promoter (forward primer: 5'GGCTGAAGCAGGAGAATCAC3' and reverse primer 5'GCTGAGTCCCAGCTGTTTTT3'. For each condition (Input, AhR ChIP and Mock ChIP), a non-treated control sample was used as a reference. The amount of the target gene (AQP3) in TCDD-treated cells, relative to the reference (NT sample), was calculated by the equation $2^{-\Delta\Delta Ct}$ where ΔCt = (Ct TCDD sample - Ct reference NT sample). The equation thus represents the expression of the target gene in the TCDD-treated sample relative to its expression in the NT sample.

Preparation of RNA and Reverse Transcription quantitative PCR

For most experiments, 0.2 million cells were seeded into 6-well plates and treated, or not, 2 days later with the compounds indicated in the figures (TCDD, Benzo(a)pyrene, 3-methylcholanthrene, resveratrol and quercetin). RNA was prepared using the RNeasy mini kit from Qiagen (France). Reverse transcription was performed using the High Capacity cDNA Reverse Transcription Kit (Life technology, France) as described. Then quantitative PCR was performed with 40 ng of cDNA as described previously, with duplicates for each experiment. The human primers were: RPL13A forward 5'-AAGGTCGTGCGTCTGAAG-3' and reverse 5'-GAGTCCGTGGGTCTTGAG-3', AQP3 forward 5'-GCAGCCTGTCCATCTGTG-3' and reverse 5'-ACCCTACTTCCCAAAAGCC-3'. The mouse primers were: AQP3 forward 5'-AACCCTGCTGTGACCTTTG-3' and reverse 5'-GCTGCTGTGCCTATGAACTG-3', CYP1A1 forward 5'-CCGTATTCTGCCTTGGATTC-3' and reverse 5'- CCTGCTTGATGGTGTTCAG-3' and GAPDH forward 5'- AACGACCCCTTCATTGAC -3' and reverse 5'-

TCCACGACATACTCAGCAC-3'. The relative amounts of mRNA were estimated using the delta-delta Ct method with RPL13A as the reference for human samples and glyceraldehyde 3-phosphate dehydrogenase (GAPDH) for the murine samples.

Western blot.

Cells were scraped into M-PER® Mammalian Protein Extraction Reagent containing a protease and phosphatase inhibitor cocktail (Sigma) and clarified by centrifugation. For western blots, equal amounts of total protein were separated by SDS–PAGE and transferred onto nitrocellulose membranes. Blocking of the membrane was done in 0.2% I-Block (life technologies) solution containing 0.1% Tween-20 for 1 h at room temperature followed by incubation overnight at 4°C with primary antibodies AQP3 (Ab125219, Abcam Paris, France) and actin (loading control, ab8226, Abcam Paris, France). After 3 washes with 0.1% Tween-20 PBS, the membrane was incubated with the corresponding alkaline phosphatase-conjugated secondary antibody or IRdye 800 and IRdye 680 (Sciencetec). After the final washes, signals were assessed using the *Odyssey*® Infrared Imager (LI-COR).

Transfection with siRNA

One day before transfection, HepG2 cells (4.10^5 cells per well) were seeded into 6-well plates. Twenty-four hours later, the medium was replaced by DMEM without phenol red supplemented with 3% charcoal-treated (desteroidized) calf serum and cells were then transfected with 5 nM siRNA, using the HiPerfect transfection reagent (Qiagen) according to the manufacturer's protocol. For experiments involving AQP3, after 8 h of incubation at 37°C, the medium was replaced and the cells were treated or not with 25 nM TCDD. Seventy-two hours after transfection, purification of RNA

and examination of thecellular immunofluorescence were carried out. SiRNA references (Qiagen) are: Hs_AQP3_5_HP Validated siRNA (ref: SI02776900) and Hs_AQP3_6_HP Validated siRNA (ref: SI02780295).

Immunofluorescence

Cells were seeded onto glass coverslips in 6-well plates at a concentration of approximately $5x10^5$ cells per well. Cells were exposed to TCDD (25 nM) for 48 h in DMEM without phenol red supplemented with 3% charcoal-treated calf serum. For immunofluorescence, all steps were carried out at room temperature.

The coverslips were washed twice with 1 X PBS and then fixed with 4% paraformadehyde for 20 min. The cells were permeabilized for 3 min with 0.3% Triton- PBS- and then incubated with 1% bovine serum albumin-PBS-, 0.3M glycine for 30 min. Incubation with the primary antibody to AQP3 (Ab125219, Abcam Paris, France) was performed for 1 h at room temperature in 1% bovine serum albumin-PBS. For staining of actin and the nucleus, FITC-conjugated phalloidin and TO-PRO-3 (Invitrogen) were included during the incubation with the secondary antibody. The coverslips were sealed with Dako Faramount Aqueous Mounting Medium Ready-to-use (Invitrogen). Mounted cells were observed and images recorded using a Zeiss LSM 510 confocal microscope (Carl Zeiss Meditec France SAS, Le Pecq, France) with a Zeiss 63x Plan-Apochromat O.N. = 1,4 / Oil / DIC objective and LSM Image Browser.

xCELLigence Real-Time Cell Analysis (RTCA) of Migration

Cell migration was carried out using an xCELLigence RTCA DP instrument (ACEA Biosciences) which was placed in a humidified incubator at 37 °C and 5% CO_2. The

experiments were performed using modified 16-well plates (CIM-16) with each well consisting of an upper and a lower chamber separated by a microporous membrane. Microelectrodes were attached to the underside of the membrane for impedance-based detection of migrated cells.

HepG2 cells (50.000 cells per well) were seeded into CIM-16 plates (which are specifically used to measure cell migration) in DMEM without phenol red supplemented with 3% charcoal-treated (desteroidized) calf serum and were transfected with the siControl (siC) or the siAQP3 using the RNAi Max transfection reagent according to the protocol provided by the supplier (Life Technologies,Rockville, MD, USA). The lower chambers contained media with 10% FBS in order to assess chemotactic migration. After 24 h of incubation at 37 °C, the medium was replaced and the cells were treated, or not, with 25 nM TCDD. The impedance value of each well was automatically monitored by the xCELLigence system and expressed as a cell index value (CI). Higher CI values equate to more migration; the cells migrate from the upper chamber towards the lower chamber. The migration curves were monitored online of every 5 min during the 160 h of incubation and the slope of the migration curve was calculated using the RTCA 1.2 software. Each experiment was performed in triplicates.

Statistical analysis

The results arising from three independent experiments are expressed as the mean ± SD (standard deviations). Statistical analysis was performed using successively the U Mann-Whiteny's test (nonparametric comparison of 2 independent series) or H Kruskal-Wallis's test (nonparametric comparison of k

independent series) followed by a 1-factor ANOVA test (parametric comparison of k independent series). A value of $p < 0.05$ was considered statistically significant.

Results

The expression of AQP3 in mice is up regulated following exposure to TCDD exposure

Our previous studies showed that TCDD and the AhR triggered cell migration(Bui et al., 2009). In order to identify putative targets involved in this process, we screened available microarray data (from our laboratory) for changes in gene expression following treatment of cell lines with dioxin (Diry et al., 2006). The expression of AQP3 was found to be increased. Since aquaporins have been described as critical regulators of cell migration and potentially metastasis, we examined whether the expression of AQP3 is regulated by TCDD in several murine tissues. Figure 1 shows that whereas CYP1A1 (a TCDD target) expression is increased in all the organs examined (Figure 1A), the levels of AQP3 mRNA are significantly up-regulated only in skin and in liver (Figure 1B).

AQP3 mRNA and protein levels are increased by TCDD

To decipher the mechanisms involved in this regulation, we examined the kinetics and dose-response characteristics following treatment with TCDD of HepG2 cells, which express the Aryl hydrocarbon Receptor (AhR). We found an increase in AQP3 mRNA expression that was significant after 8h of exposure of cells to 25 nM TCDD treatment. This increase remained significant for longest periods of time tested (48 hours, Figure 2A) indicating that the AQP3 gene is a transcriptional target of dioxin. A significant induction of AQP3 expression was observed following exposure of cells, for either 24 or 48 hours, to concentrations of TCDD in the range of 1-100 nM (Figures 2B and 2C). The amount of AQP3 protein was significantly increased

following treatment for 24 or 48 hours with 25 nM TCDD (Figure 2D and supplementary figure 1). We demonstrated that AQP3 mRNA is increased in liver but also in skin in TCDD-exposed mice; we then checked the expression of AQP3 mRNA in the human epidermal keratinocytes derived from the foreskin of a newborn (strain YF23) (Vanhoutteghem and Djian, 2004) and demonstrated that it was significantly increased following treatment for 48 hours with 25 nM TCDD (Supplementary Figure 2)

The induction of AQP3 expression depends upon the AhR

We next investigated the involvement of the AhR in the induction of AQP3 expression. Three other AhR ligands (3MC, BaP and quercetine) were able to significantly increase the AQP3 mRNA expression albeit to different extents (Figure 3A). Resveratrol increases the level of AQP3 and blocks the effects of TCDD.

In a cell line which does not express a optimal AhR pathway (MDA-MB-231), AQP3 is not induced following exposure of cells for 48 hours to 25 nM dioxin (Figure 3B). We then used RNA interference to decrease the levels of AhR in the HepG2 cells exposed or not to TCDD (Figure 3C). Following AhR knockdown, the increase in expression of both CYP1A1 (Figure 3D) and AQP3 (Figure 3E) are significantly reduced following exposure of cells to TCDD. These results strongly suggest that the AhR is involved in mediating the effects of TCDD. Finally, using analysis by chromatin immunoprecipitation (ChIP), we found that AhR binds to the AQP3 promoter (which contains a potential XRE as identified by the MatInspector software located in -954/-950) of HepG2 cells exposed to 25nM TCDD (Figure 3F).

We then investigated the function of AQP3 in HepG2 cells, specifically when its expression is triggered by TCDD. We used RNA interference to knockdown AQP3 mRNA levels by more than 60% (Figure 4A, 75% with TCDD). The level of CYP1A1 mRNA was not modified which suggests that this knockdown is specific (Figure 4B). Immunofluorescence was then used to investigate the morphological changes induced by exposure of cells to TCDD. Antibodies to actin and paxillin were used to examine, respectively, the cytoskeleton and focal adhesion sites. Cells exposed to TCDD had dramatically altered morphologies as seen previously (cell spreading, formation of focal adhesion sites). Remarkably, transfection of cells with siAQP3 blunted this effect (Figure 4C). Finally, we investigated global cellular attributes in another way. We used the xCELLigence system with specific plates (CIM plates) to measure cell invasion and migration. Cells exposed to TCDD had CI values that significantly increased over time, which suggests that cell invasion/migration was increased (Figure 4D). The use of RNA interference to reduce the induction, by TCDD, of expression of AQP3 impairs this effect. These results suggest that the induction of AQP3 is a required step in a molecular pathway that leads to changes in liver cell morphology and migration following exposure to TCDD.

Discussion

In this study, we show that the expression of AQP3 can be regulated by the Ah Receptor (AhR), which, in turn, is activated by numerous exogenous and endogenous ligands. In line with our previous studies on Hef1 and Sos1 (Bui et al., 2009; Pierre et al., 2011; Tomkiewicz et al., 2013), this regulation of AQP3 appears also critical for the migration of cancer cells exposed to AhR ligands, suggesting that several participants in the epithelial-mesenchymal transition (EMT) are concomitantly up-regulated or activated, which leads to cellular remodeling of focal adhesion sites (HEF1, FAK, Src), cell proliferation (SOS1) and migration (AQP3) (Bui et al., 2009; Pierre et al., 2011; Tomkiewicz et al., 2013). An epithelial cell undergoes EMT when it loses its epithelial markers and acquires mesenchymal markers; as a consequence, adhesion and migration properties are changed. EMT has been described in physiological (gastrulation) and pathological (fibrosis) processes and is suspected to be involved in the formation of metastatic cells.

AQP3 is expressed in epithelia (oral, mammary gland) (Poveda et al., 2014; Mobasheri and Barrett-Jolley, 2014). Its expression has been shown to be regulated not only by a number of physiological stimuli including Epidermal Growth Factor (EGF) or Hepatocyte Growth Factor (HGF) but also by cellular regulatory processes such as miRNA production (miR-874) (Jiang et al., 2014; Zhi et al., 2014). The up-regulation of AQP3 may be also related to epithelial-mesenchymal transition since AQP3 modulates cell migration and invasion and decreases the expression of E-Cadherin through activation of the PI3K (phosphoinositide 3-kinase)/AKT/SNAIL pathway (Chen et al., 2015). The mechanism linking AQP3 to the PI3K pathway remains to be characterized.

AQP3 has been implicated in the regulation of cell migration in other systems. For example, a recent study using human skin samples showed that the expression of AQP3 increased following burn injury, specifically along the burn edge and that this expression contributes to burn healing (Sebastian et al., 2015). Interestingly, it might be possible that a burn injury produces locally some polycyclic aromatic hydrocarbons which could activate the AhR and then induce AQP3. Peritoneal wound healing also depends on the expression of AQP3 which is, in this specific case, stimulated by transforming growth factor beta 1 (TGF-ß1), whose expression is also stimulated upon TCDD exposure in mice (Ryu et al., 2012; Pierre et al., 2014).

The regulation of cell migration is also a critical process in the appearance of metastatic cells and AQP3 has been implicated in the migration of cancer cells using different models. This is the case for human mammary (stimulated by fibroblast growth factor 2) (Cao et al., 2013), gastric (stimulated by c-Met or EGD) (Wang et al., 2012; Xu et al., 2011; Huang et al., 2010) colon and pancreatic cell lines (stimulated by EGF). These studies have been helpful showing that the PI3K/AKT and ERK (Extracellular signal-Regulated Kinase 1/2) pathways are involved in the up-regulation of the expression of AQP3. For example, the knockdown of AQP3 mRNA and protein in prostate cancer cell lines leads to a reduction of ERK1/2 signaling and MMP3 (Matrix Metalloprotease 3) secretion (Chen et al., 2015).

Taking into consideration the diverse physiological and pathophysiological processes involving AQP3, we hypothesize that the regulation of this protein by the Aryl hydrocarbon Receptor (AhR) might be critical for AhR ligand-related pathologies including chloracne (a skin disease highly related to dioxin exposure), metabolic disorders (due to its expression in adipose tissues) and cancer. In particular, we hypothesize that AQP3 increases water transport at the proximity of the cell

membrane thus allowing a reshaping of cellular protrusions, which are essential for cell migration. Ji C. et al (Ji et al., 2008), showed that curcumin, an AhR ligand, impairs both the induction of AQP3 and cell migration in human ovarian CaOV3 cells. This is coherent with our hypothesis that each AhR ligand acts differently on the AhR; although the authors demonstrated that curcumin blocks the EGF pathway, it is also possible that it inhibits AhR signaling as this polyphenol is described as an antagonist of TCDD (Gouédard et al., 2003, 2004; Guyot et al., 2012, 2013; Juricek et al., 2014). The regulation of AQP3 by the AhR might be even more complex, while taking in account the interplay between the receptor and the estrogen pathway. Indeed, Boverhof et al., studied the inhibition of estrogen-mediated uterine gene expression responses by TCDD and show that ethinyl estradiol (EE) blocks Aqp3 mRNA expression in mice in the uterus (Boverhof et al., 2008). Moreover, Burns et al, showed that exposure to TCDD during gestation, also blunted the adult uterine response to estradiol in mice; as a consequence, E2-induction of Aqp3 mRNA is also decreased by TCDD (Burns et al., 2013). Both studies strongly suggest that AQP3 is a target gene of the estrogen receptors (ER) and the aryl hydrocarbon receptor pathways. Interestingly, TCDD has been shown to display both pro-estrogenic or anti-estrogenic properties according to the presence of estradiol, the tissue and the context (ex: pro-estrogenic in case of an unbound state) (Ohtake et al., 2003). One hypothesis would be that estrogen-responsive tissues positively responds to estradiol and negatively to TCDD regarding AQP3 (and probably other genes), while tissues such as skin or liver only respond to TCDD (but possibly in a complex involving the unbound ER).

Cancer phenotypes are dependent on the inflammatory and hypoxic characteristics of the tumor which also have been associated with the expression of AQP3. A recent study showed that AQP3 might be important in the regulation of inflammation: AQP3 is transcriptionally regulated by Notch signaling in keratinocytes. The Notch-AQP3 pathway (which involves a negative feedback loop) triggers the production of pro-inflammatory cytokines and its dysregulation is associated with the development of skin cancers (Guo et al., 2013). Moreover, the overexpression of several AQPs in PC12 cells (rat pheochromocytoma) leads to the stabilization of Hypoxia Induced Factor-2 alpha (HIF-2 alpha), a transcription factor which positively regulates angiogenesis, glucose metabolism and the acquisition of invasive properties (Galán-Cobo et al., 2013). HIF-2 alpha acts through binding to ARNT, the transcriptional partner of the AhR.

In conclusion, we provide here the first evidence for a link between an environmental insult and the up-regulation of expression of AQP3. While important from a toxicological point of view, there also may be pharmacological implications. Manipulation of the AhR pathway (using agonists or antagonists of the receptor) to increase or decrease the expression of AQP3 may be useful for skin (re)-hydration, wound healing and for regulating cancer progression.

Conflict of interest

The authors declare no conflict of interest

Funding information

This work was supported by ANSES (Agence Nationale de la Sécurité, de l'Environnement et de la Santé; all of the authors); ANR (Agence Nationale de la Recherche, 06SEST26, ONCOPOP; all of the authors); ARC (Association pour la Recherche sur le Cancer, 3927 & SFI20101201842; all of the authors); the Assistance Publique-Hôpitaux de Paris (Robert Barouki) ; CNRS (Centre National de la Recherche Scientifique); Fondation pour la Recherche Medicale (Postdoctoral fellowship, Linh-Chi Bui); the Hospital « Européen Georges Pompidou » and « Necker Enfants Malades » ; INSERM (Institut National de la Santé et de la Recherche Médicale; all of th authors); Ligue contre le Cancer (Postdoctoral fellowship, Linh-Chi Bui); ComUE Sorbonne Paris Cité ; Université Paris Descartes.

Acknowledgments

We thank Dr. Lawrence Aggerbeck for his critical reading of this manuscript and Dr. Philippe Djian who gave us the YF23 strain (CNRS UMR8118 - Université Paris Descartes).

References

Barouki R, Coumoul X (2010) Cell migration and metastasis markers as targets of environmental pollutants and the Aryl hydrocarbon receptor. Cell Adhes Migr 4:72–76.

Barouki R, Coumoul X, Fernandez-Salguero PM (2007) The aryl hydrocarbon receptor, more than a xenobiotic-interacting protein. FEBS Lett 581:3608–3615.

Boverhof DR, Burgoon LD, Williams KJ, Zacharewski TR (2008) Inhibition of estrogen-mediated uterine gene expression responses by dioxin. Mol Pharmacol 73:82–93.

Bui L-C, Tomkiewicz C, Chevallier A, Pierre S, Bats A-S, Mota S, Raingeaud J, Pierre J, Diry M, Transy C, Garlatti M, Barouki R, Coumoul X (2009) Nedd9/Hef1/Cas-L mediates the effects of environmental pollutants on cell migration and plasticity. Oncogene 28:3642–3651.

Burns KA, Zorrilla LM, Hamilton KJ, Reed CE, Birnbaum LS, Korach KS (2013) A single gestational exposure to 2,3,7,8-tetrachlorodibenzo-p-dioxin disrupts the adult uterine response to estradiol in mice. Toxicol Sci Off J Soc Toxicol 136:514–526.

Cao X-C, Zhang W-R, Cao W-F, Liu B-W, Zhang F, Zhao H-M, Meng R, Zhang L, Niu R-F, Hao X-S, Zhang B (2013) Aquaporin3 is required for FGF-2-induced migration of human breast cancers. PloS One 8:e56735.

Carvajal-Gonzalez JM, Roman AC, Cerezo-Guisado MI, Rico-Leo EM, Martin-Partido G, Fernandez-Salguero PM (2009) Loss of dioxin-receptor expression

accelerates wound healing in vivo by a mechanism involving TGFbeta. J Cell Sci 122:1823–1833.

Chen J, Wang Z, Xu D, Liu Y, Gao Y (2015) Aquaporin 3 promotes prostate cancer cell motility and invasion via extracellular signal-regulated kinase 1/2-mediated matrix metalloproteinase-3 secretion. Mol Med Rep 11:2882–2888.

Coumoul X, Diry M, Robillot C, Barouki R (2001) Differential regulation of cytochrome P450 1A1 and 1B1 by a combination of dioxin and pesticides in the breast tumor cell line MCF-7. Cancer Res 61:3942–3948.

Diry M, Tomkiewicz C, Koehle C, Coumoul X, Bock KW, Barouki R, Transy C (2006) Activation of the dioxin/aryl hydrocarbon receptor (AhR) modulates cell plasticity through a JNK-dependent mechanism. Oncogene 25:5570–5574.

Galán-Cobo A, Sánchez-Silva R, Serna A, Abreu-Rodríguez I, Muñoz-Cabello AM, Echevarría M (2013) Cellular overexpression of aquaporins slows down the natural HIF-2α degradation during prolonged hypoxia. Gene 522:18–26.

Gouédard C, Barouki R, Morel Y (2004) Dietary polyphenols increase paraoxonase 1 gene expression by an aryl hydrocarbon receptor-dependent mechanism. Mol Cell Biol 24:5209–5222.

Gouédard C, Koum-Besson N, Barouki R, Morel Y (2003) Opposite regulation of the human paraoxonase-1 gene PON-1 by fenofibrate and statins. Mol Pharmacol 63:945–956.

Guo L, Chen H, Li Y, Zhou Q, Sui Y (2013) An aquaporin 3-notch1 axis in keratinocyte differentiation and inflammation. PloS One 8:e80179.

Ji C, Cao C, Lu S, Kivlin R, Amaral A, Kouttab N, Yang H, Chu W, Bi Z, Di W, Wan Y (2008) Curcumin attenuates EGF-induced AQP3 up-regulation and cell migration in human ovarian cancer cells. Cancer Chemother Pharmacol 62:857–865.

Jiang B, Li Z, Zhang W, Wang H, Zhi X, Feng J, Chen Z, Zhu Y, Yang L, Xu H, Xu Z (2014) miR-874 Inhibits cell proliferation, migration and invasion through targeting aquaporin-3 in gastric cancer. J Gastroenterol 49:1011–1025.

Ma C, Marlowe JL, Puga A (2009) The aryl hydrocarbon receptor at the crossroads of multiple signaling pathways. EXS 99:231–257.

Ohtake F, Takeyama K, Matsumoto T, Kitagawa H, Yamamoto Y, Nohara K, Tohyama C, Krust A, Mimura J, Chambon P, Yanagisawa J, Fujii-Kuriyama Y, Kato S (2003) Modulation of oestrogen receptor signalling by association with the activated dioxin receptor. Nature 423:545–550.

Pierre S, Bats A-S, Chevallier A, Bui L-C, Ambolet-Camoit A, Garlatti M, Aggerbeck M, Barouki R, Coumoul X (2011) Induction of the Ras activator Son of Sevenless 1 by environmental pollutants mediates their effects on cellular proliferation. Biochem Pharmacol 81:304–313.

Pierre S, Chevallier A, Teixeira-Clerc F, Ambolet-Camoit A, Bui L-C, Bats A-S, Fournet J-C, Fernandez-Salguero P, Aggerbeck M, Lotersztajn S, Barouki R, Coumoul X (2014) Aryl hydrocarbon receptor-dependent induction of liver fibrosis by dioxin. Toxicol Sci Off J Soc Toxicol 137:114–124.

Poveda M, Hashimoto S, Enokiya Y, Matsuki-Fukushima M, Sasaki H, Sakurai K, Shimono M (2014) Expression and localization of aqua-glyceroporins AQP3 and AQP9 in rat oral epithelia. Bull Tokyo Dent Coll 55:1–10.

Rey-Barroso J, Alvarez-Barrientos A, Rico-Leo E, Contador-Troca M, Carvajal-Gonzalez JM, Echarri A, Del Pozo MA, Fernandez-Salguero PM (2014) The Dioxin receptor modulates Caveolin-1 mobilization during directional migration: role of cholesterol. Cell Commun Signal CCS 12:57.

Rico-Leo EM, Alvarez-Barrientos A, Fernandez-Salguero PM (2013) Dioxin receptor expression inhibits basal and transforming growth factor β-induced epithelial-to-mesenchymal transition. J Biol Chem 288:7841–7856.

Ryu H-M, Oh E-J, Park S-H, Kim C-D, Choi J-Y, Cho J-H, Kim I-S, Kwon T-H, Chung H-Y, Yoo M, Kim Y-L (2012) Aquaporin 3 expression is up-regulated by TGF-β1 in rat peritoneal mesothelial cells and plays a role in wound healing. Am J Pathol 181:2047–2057.

Sebastian R, Chau E, Fillmore P, Matthews J, Price LA, Sidhaye V, Milner SM (2015) Epidermal aquaporin-3 is increased in the cutaneous burn wound. Burns J Int Soc Burn Inj.

Tomkiewicz C, Herry L, Bui L-C, Métayer C, Bourdeloux M, Barouki R, Coumoul X (2013) The aryl hydrocarbon receptor regulates focal adhesion sites through a non-genomic FAK/Src pathway. Oncogene 32:1811–1820.

Vanhoutteghem A, Djian P (2004) Basonuclin 2: an extremely conserved homolog of the zinc finger protein basonuclin. Proc Natl Acad Sci U S A 101:3468–3473.

Verkman AS, Anderson MO, Papadopoulos MC (2014) Aquaporins: important but elusive drug targets. Nat Rev Drug Discov 13:259–277.

Wang J, Gui Z, Deng L, Sun M, Guo R, Zhang W, Shen L (2012) c-Met upregulates aquaporin 3 expression in human gastric carcinoma cells via the ERK signalling pathway. Cancer Lett 319:109–117.

Zhi X, Tao J, Li Z, Jiang B, Feng J, Yang L, Xu H, Xu Z (2014) MiR-874 promotes intestinal barrier dysfunction through targeting AQP3 following intestinal ischemic injury. FEBS Lett 588:757–763.

Figures legends

Figure 1: Dioxin treatment increases the level AQP3 mRNA *in vivo* in the skin and the liver

Wild-type mice were treated on days 0 and 7, with either TCDD (25 µg/kg) or corn oil (control) and sacrificed on day 14. CYP1A1 (A) and AQP3 (B) mRNA levels were measured by quantitative real time PCR (qRT-PCR). The single and triple asterisks indicate $P < 0.05$ and $P < 0.001$, respectively, as compared to controls.

Figure 2: Dioxin treatment increases the levels of AQP3 mRNA and protein *in vitro* in HepG2 cells. The levels of AQP3 mRNA and protein were measured by quantitative real-time PCR (A, B, C) and Western blot (D) in time-course (A, D) and dose-response (B, C) studies of dioxin-treated cells. The single and double asterisks indicate $P < 0.05$ and $P < 0.01$, respectively, as compared to the control condition.

Figure 3: The AhR regulates the transcription of AQP3

(A) Quantitative real-time PCR measurement of the level of AQP3 mRNA following48 h of exposuret of HepG2 cells to AhR ligands (3MC: 3-methylcholanthrene; BaP: benzo(a)pyrene). (B) Quantitative real-time PCR measurement of the level of AQP3 mRNA following exposure to ligands for 48 h of MDA-MB-231 AhR deficient cells. (C-E) Quantitative real-time PCR measurement of the levels of AhR (C), CYP1A1 (D) and AQP3 (E) mRNA in AhR small-interfering RNA (siRNA)-transfected HepG2 cells. (F) Chromatin immunoprecipitation carried out on the AQP3 promoter XRE region. Values are expressed as the mean±s.e.m. The single, double and triple asterisks

indicate $P < 0.05$, $P < 0.01$ and $P < 0.001$, respectively, as compared to the control condition.

Figure 4: AQP3 is involved in dioxin-induced changes of cell morphology and migration

(A-B) Quantitative real-time PCR measurement of the levels of AQP3 (A) and CYP1A1 (B) mRNA in AQP3 small interfering RNA (siRNA)-transfected HepG2 cells. Control siRNA (siC) was used as control and dioxin (25 nM) was used to induce AQP3. The results expressed are the mean ± s.e.m of at least three different experiments. The double and triple asterisks indicate $P < 0.01$ and $P < 0.001$, respectively, as compared to the controls. (C) Immunofluorescence microscopy showing the fluorescence of actin (green, upper part of the panel) or paxillin (red, middle part of the panel) of siRNA-transfected HepG2 cells treated or not with dioxin (25nM). The merged images are shown in the lower panel. siAQP3 transfection significantly reduces the morphological changes (cell spreading and formation of focal adhesion sites) observed following exposure of the cells to dioxin. Scale bar, 10 µm. (D) Assessment of global cell parameters (cell invasion and migration) in AQP3 small interfering RNA (siRNA)-transfected HepG2 cells following exposure of cells to dioxin made with the xCelligence system (CIM plate). The slope, represents the rate of change of the cell index as a function of time between 76h and 96h. Higher CI values equate to more migration. The results are expressed as the mean±s.e.m of at least three different experiments. The single and double asterisks indicate $P < 0.05$ and $P < 0.01$, respectively, as compared to the controls.

Supplementary Figure 1: Dioxin treatment increases the levels of AQP3 protein *in vitro* in HepG2 cells. A representative Western blot of AQP3 protein induction (time-course studies of dioxin-treated cells) is shown.

Supplementary Figure 2: Dioxin treatment increases the levels of AQP3 mRNA *in vitro* in the human epidermal keratinocytes YF23. The levels of AQP3 mRNA were measured by quantitative real-time PCR of dioxin-treated cells. The single asterisk indicates $P < 0.05$ as compared to the control condition.

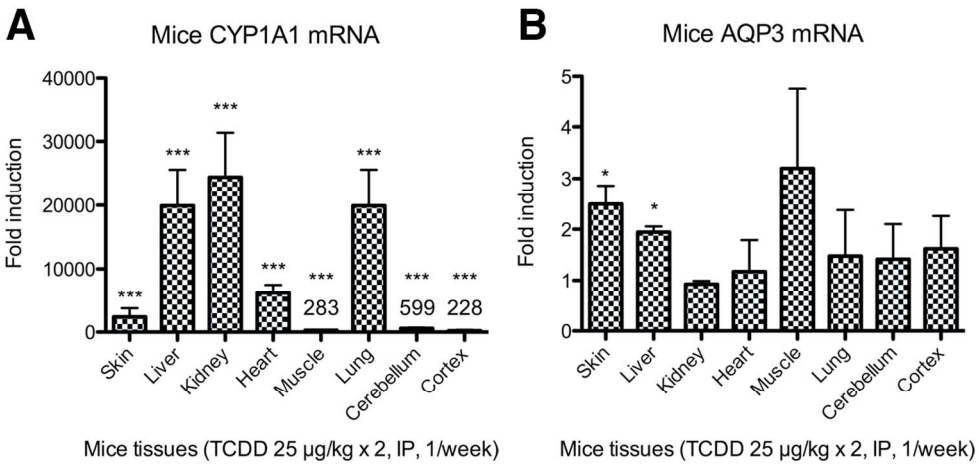

Figure 1: Dioxin treatment increases the level AQP3 mRNA in vivo in the skin and the liver
Wild-type mice were treated on days 0 and 7, with either TCDD (25 µg/kg) or corn oil (control) and sacrificed on day 14. CYP1A1 (A) and AQP3 (B) mRNA levels were measured by quantitative real time PCR (qRT-PCR). The single and triple asterisks indicate $P < 0.05$ and $P < 0.001$, respectively, as compared to controls.

127x63mm (300 x 300 DPI)

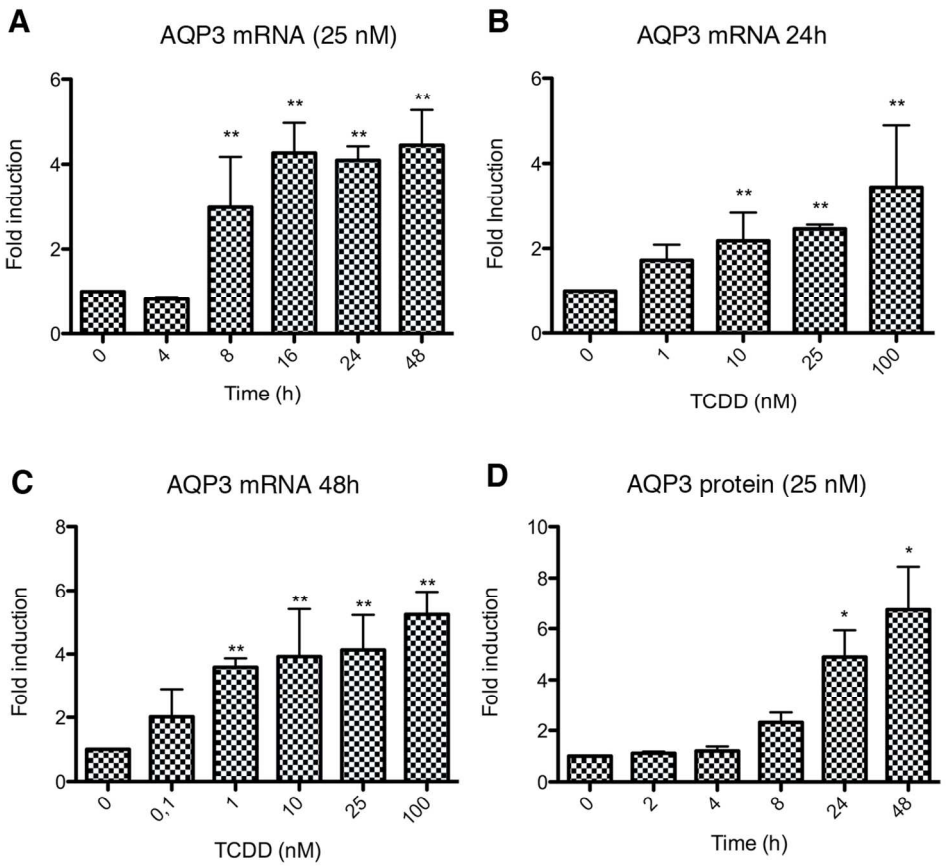

Figure 2: Dioxin treatment increases the levels of AQP3 mRNA and protein in vitro in HepG2 cells. The levels of AQP3 mRNA and protein were measured by quantitative real-time PCR (A, B, C) and Western blot (D) in time-course (A, D) and dose-response (B, C) studies of dioxin-treated cells. The single and double asterisks indicate $P < 0.05$ and $P < 0.01$, respectively, as compared to the control condition.

127x114mm (300 x 300 DPI)

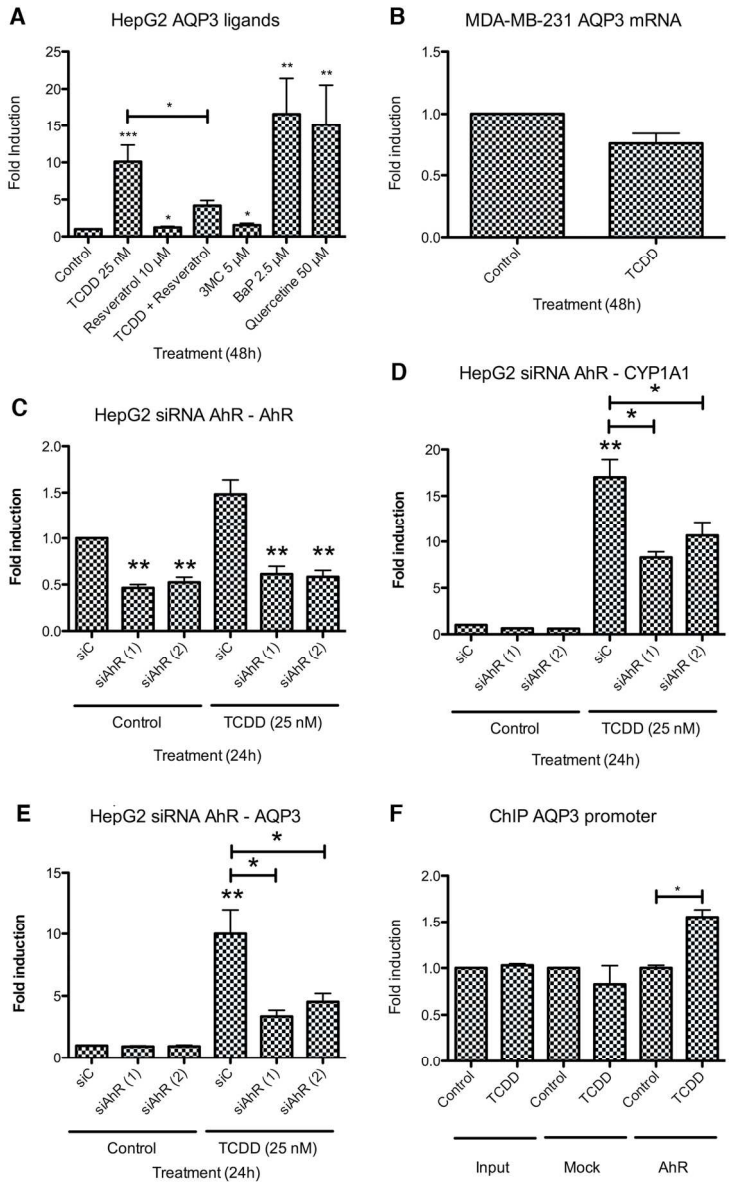

Figure 3: The AhR regulates the transcription of AQP3
(A) Quantitative real-time PCR measurement of the level of AQP3 mRNA following48 h of exposuret of HepG2 cells to AhR ligands (3MC: 3-methylcholanthrene; BaP: benzo(a)pyrene). (B) Quantitative real-time PCR measurement of the level of AQP3 mRNA following exposure to ligands for 48 h of MDA-MB-231 AhR deficient cells. (C-E) Quantitative real-time PCR measurement of the levels of AhR (C), CYP1A1 (D) and AQP3 (E) mRNA in AhR small-interfering RNA (siRNA)-transfected HepG2 cells. (F) Chromatin immunoprecipitation carried out on the AQP3 promoter XRE region. Values are expressed as the mean±s.e.m. The single, double and triple asterisks indicate $P < 0.05$, $P < 0.01$ and $P < 0.001$, respectively, as compared to the control condition.

127x199mm (300 x 300 DPI)

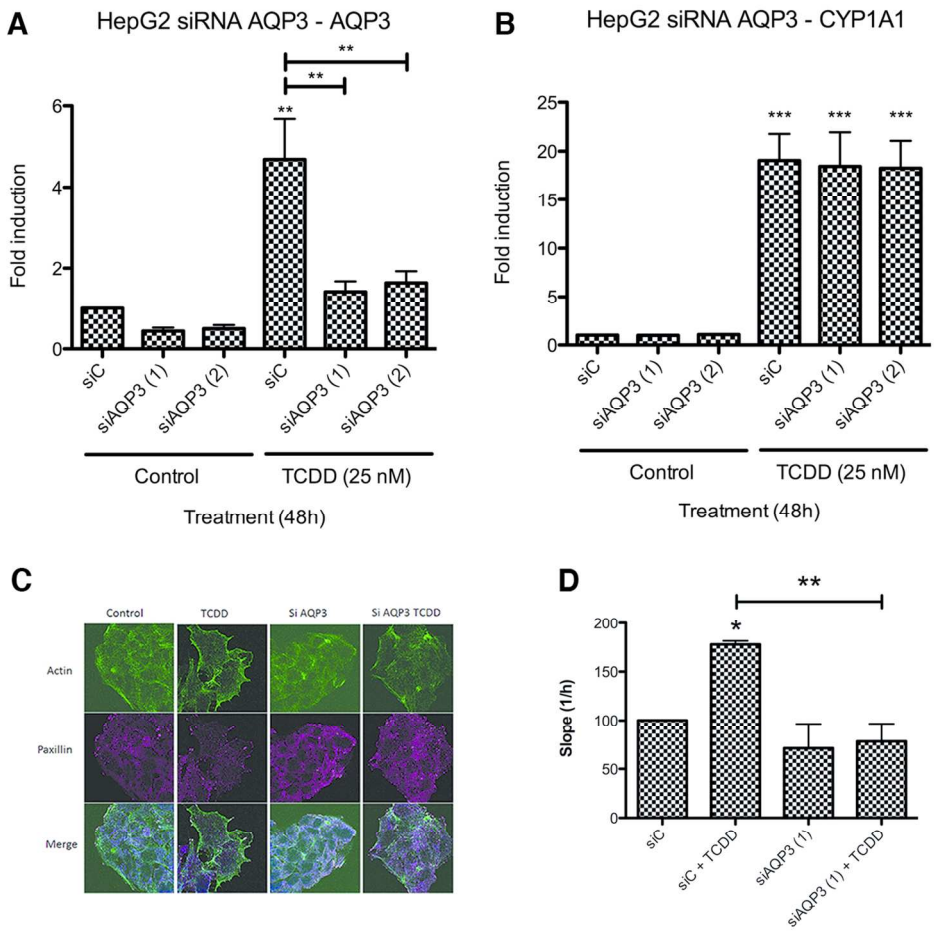

Figure 4: AQP3 is involved in dioxin-induced changes of cell morphology and migration
(A-B) Quantitative real-time PCR measurement of the levels of AQP3 (A) and CYP1A1 (B) mRNA in AQP3 small interfering RNA (siRNA)-transfected HepG2 cells. Control siRNA (siC) was used as control and dioxin (25 nM) was used to induce AQP3. The results expressed are the mean ± s.e.m of at least three different experiments. The double and triple asterisks indicate $P < 0.01$ and $P < 0.001$, respectively, as compared to the controls. (C) Immunofluorescence microscopy showing the fluorescence of actin (green, upper part of the panel) or paxillin (red, middle part of the panel) of siRNA-transfected HepG2 cells treated or not with dioxin (25nM). The merged images are shown in the lower panel. siAQP3 transfection significantly reduces the morphological changes (cell spreading and formation of focal adhesion sites) observed following exposure of the cells to dioxin. Scale bar, 10 µm. (D) Assessment of global cell parameters (cell invasion and migration) in AQP3 small interfering RNA (siRNA)-transfected HepG2 cells following exposure of cells to dioxin made with the xCelligence system (CIM plate). The slope, represents the rate of change of the cell index as a function of time between 76h and 96h. Higher CI values equate to more migration. The results are expressed as the mean±s.e.m of at least three different experiments. The single and double asterisks indicate $P < 0.05$ and $P < 0.01$, respectively, as compared to the controls.

127x120mm (300 x 300 DPI)